26. Soloviev, M. M. & Barnard, E. A. *Xenopus* oocytes express a unitary glutamate receptor endogenously. *J. Mol. Biol.* **273,** 14–18 (1997).

27. Ishimaru, H. *et al.* A unitary non-NMDA receptor short subunit from *Xenopus*: DNA cloning and expression. *Receptors Channels* **4,** 31–49 (1996).

28. von Euler, M., Li-Li, M., Whittemore, S., Seiger, A. & Sundström, E. No protective effect of the NMDA antagonist memantine in experimental spinal cord injuries. *J. Neurotrauma* **14,** 53–61 (1997).

29. Paleček, J., Abdrachmanova, G., Vlachová, V. & Vyklický, L. Jr Properties of NMDA receptors in rat spinal cord motoneurons. *Eur. J. Neurosci.* **11,** 827–836 (1999).

30. Souverbie, F., Mo, L.-L., Liu, Y., von Euler, G. & Sundström, E. Pharmacological characterization of [³H]MK-801 binding in the rat spinal cord. *Eur. J. Pharmacol.* **307,** 347–353 (1996).

....

Establishment of developmental precision and proportions in the early *Drosophila* embryo

Bahram Houchmandzadeh*†**, Eric Wieschaus*** **& Stanislas Leibler***‡§

* *Howard Hughes Medical Institute, Department of Molecular Biology, Princeton University, Princeton, New Jersey 08544, USA*
† *CNRS, Laboratoire de Spectrometrie Physique, BP87, 38402, St-Martin D'Heres Cedex, France*
‡ *Department of Physics, Princeton University, Princeton, New Jersey 08544, USA*

....

During embryonic development, orderly patterns of gene expression eventually assign each cell in the embryo its particular fate. For the anteroposterior axis of the *Drosophila* embryo, the first step in this process depends on a spatial gradient of the maternal morphogen Bicoid (Bcd). Positional information of this gradient is transmitted to downstream gap genes, each occupying a well defined spatial domain[1–4]. We determined the precision of the initial process by comparing expression domains in different embryos. Here we show that the Bcd gradient displays a high embryo-to-embryo variability, but that this noise in the positional information is strongly decreased ('filtered') at the level of *hunchback* (*hb*) gene expression. In contrast to the Bcd gradient, the *hb* expression pattern already includes the information about the scale of the embryo. We show that genes known to interact directly with Hb are not responsible for its spatial precision, but that the maternal gene *staufen* may be crucial.

Development is a precise process. All biochemical phenomena are prone to variation; at each level, correcting mechanisms should exist to avoid the transmission of errors and their amplification to downstream genes. The establishment of a morphogen gradient is a good example of an error-prone process. The morphogen gradient model[1] is the most widely accepted model describing how cells in early embryos acquire their positional information: because the concentration of a morphogen decreases with the distance from one pole, measuring this concentration informs a cell of its position inside the embryo. In *Drosophila* embryos, the maternal gene *bcd* possesses many properties of a prototypical morphogen[2–4]. In such models, downstream genes, such as *hb*, are activated by a 'threshold' mechanism: only cells that measure concentrations of Bcd above a certain level switch on the *hb* gene.

It is hard to imagine how precision could be achieved in this simple threshold model. To produce exactly the same concentration profile of Bcd in each embryo, the mother would have to control the exact amount of messenger RNA deposited in each embryo, its localization, and the amount of protease responsible for the morphogen degradation. Any error in these parameters modifies the morphogen gradient and induces error in the positional information delivered to downstream genes[5]. Even if these parameters were precisely controlled, the gradient profile would still be sensitive to environmental conditions such as temperature. Another limitation of a simple gradient is conservation of proportions: an exponential gradient has its own length scale λ (depending on the diffusion coefficient D and the protein degradation rate ω, $\lambda^2 = D/\omega$), which is independent of the length of the embryo.

We address here both the issue of the error in the positional information of the Bcd gradient and the establishment of the spatial proportions in the embryo. To quantify the precision of gene expression, we measured protein profiles at cycle 14 by immunofluorescence staining (Fig. 1, see Methods). The Bcd protein profiles in about 100 wild-type embryos during early cycle 14 (before significant membrane invagination) are shown in Fig. 2a. The profile displays a high embryo-to-embryo variability. To quantify this variability, we measured the position (x_{Bcd}) along the embryo at which each curve crosses a certain threshold (t), chosen here as 0.23 of the maximal intensity (see Methods). These positions are spread over 30% of the embryonic length (EL) (Fig. 2b), and have a standard deviation (σ_{Bcd}) of 0.07 EL. This means that the positional error of the Bicoid gradient is greater than five nuclei in 50% of embryos. Another way to quantify the variability, which is not sensitive to the normalization of the Bcd protein profile, is to measure the slope of the exponential decay of each curve, λ (Fig. 2c). The standard deviation of λ is 0.045 EL, which corresponds to the
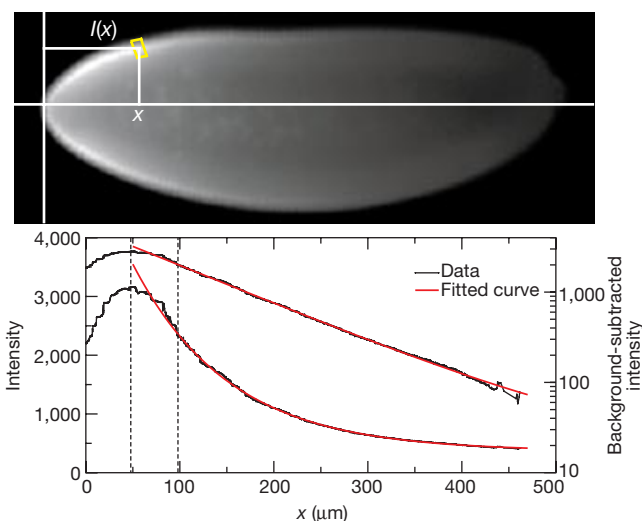

Figure 1 Typical image of Bcd staining, and the profile of the extracted curve. For Bcd, profiles are fitted well by an exponential decay. Right axis, intensity in a linear scale; left axis, background-subtracted intensity in log scale. The size of the area used to compute the intensity is exaggerated (see Methods).

same variability we measured for x_{Bcd} ($\sigma_{Bcd} = \sigma_\lambda \ln(1/t)$).

In contrast to Bcd, the Hb protein profile displays an extreme reproducibility from embryo to embryo. The Hb profile in about 100 embryos from early to late cycle 14 is shown in Fig. 2d. We quantified the *hb* distribution using the point (x_{Hb}) at which each profile crosses the 0.5 threshold (Fig. 2b). The standard deviation of x_{Hb} (σ_{Hb}) is 0.01 EL, meaning that two-thirds of embryos have Hb boundaries defined more precisely than the size of one nucleus. The information about the embryo scale is also revealed at *hb* expression level. As discussed above, the Bicoid exponential profile should not be affected by embryo length. When x_{Bcd} is plotted against EL (Fig. 2e), the correlation coefficient is indeed negligible ($P = 0.40$). A similar lack of correlation is observed between the values of λ and EL. In contrast to Bcd, however, the position of the Hb boundary displays a strong correlation with the embryo length (Fig. 2f). The linear (r) and Spearman's rank (r_s) correlation coefficients between x_{Hb} and EL are 0.84 and 0.82, respectively ($P < 10^{-20}$; all *P*-values are computed for r_s). *hb* mRNA displays the same precision and conservation of proportions as Hb protein. The spatial position of the *hb* mRNA boundary in early cycle 14 embryos has a standard deviation of 0.01 EL, and displays a high correlation with the egg length ($r_s = 0.88$, $P < 10^{-8}$).

The precision of the Hb boundary compared with the variability of the Bcd gradient could seem at odds with experiments where Bcd dosage has been modified. However, when the Hb boundary position as a function of Bcd dosage is compared with the expected value from a simple threshold model (Table 1), the measured shift is significantly smaller than that expected, even when the reduced efficiency we measure for the *bcd* transgenes is taken into consid-

Table 1 Hb boundaries in different *bcd* backgrounds

Background	Measured	Expected if efficiency is 50%	Expected if efficiency is 100%
x_{Hb} (*bcd* 1×)	0.41	NA	0.30
x_{Hb} (*bcd* wild type)	0.49	NA	NA
x_{Hb} (*bcd* 4×)	0.56	0.60	0.68
x_{Hb} (*bcd* 6×)	0.59	0.68	0.79

The measured and expected values for the position of the Hb boundary are shown for different *bcd* dosages. The expected shift of Hb boundary is $\lambda\ln(n/n_0)$, where *n* is the number of copies of *bcd* compared with the wild type ($n_0 = 2$). The σ_{Hb} is 1% for the wild-type embryos and *bcd* 1×, 1.5% for *bcd* 4×, and 2% for *bcd* 6×. The statistical significance of the differences between the expected and measured x_{Hb}, $P < 10^{-16}$. For 4× and 6×, flies carrying two copies of a *bcd* transgene on chromosome X were used. Heterozygous mothers have four copies of *bcd* (*bcd* 4×) and homozygous ones possess six copies (*bcd* 6×). For 1×, mothers heterozygous for *bcd*[E1] were used. *bcd* wild-type flies are 2×. NA, not applicable.

eration. The shift cannot be explained quantitatively if *hb* were activated only by Bicoid.

In mid-embryo, the Hb concentration decreases from the highest to the lowest value across about 0.1 EL. The corresponding change in Bcd concentration in this region is only 30% (corresponding to $1 - \exp(-0.1/0.27)$). If Bcd were the only source of cooperative activation of *hb*, this small change in the Bcd concentration would necessitate a Hill coefficient of more than 10. Such strong cooperative activation would be very sensitive to temperature variations[6]. To measure the temperature sensitivity of the Hb profile, we collected embryos for 1 h at 25 °C, and then allowed them to reach cycle 14 at different temperature (9–29 °C). The developmental time varies strongly as a function of temperature, and ranges from 2 h at 25 °C to 20 h at 9 °C. The induced changes in the Bcd and Hb profiles are shown in Fig. 3c and d. The Bcd profile is sensitive to temperature: this could be expected from a simple diffusing
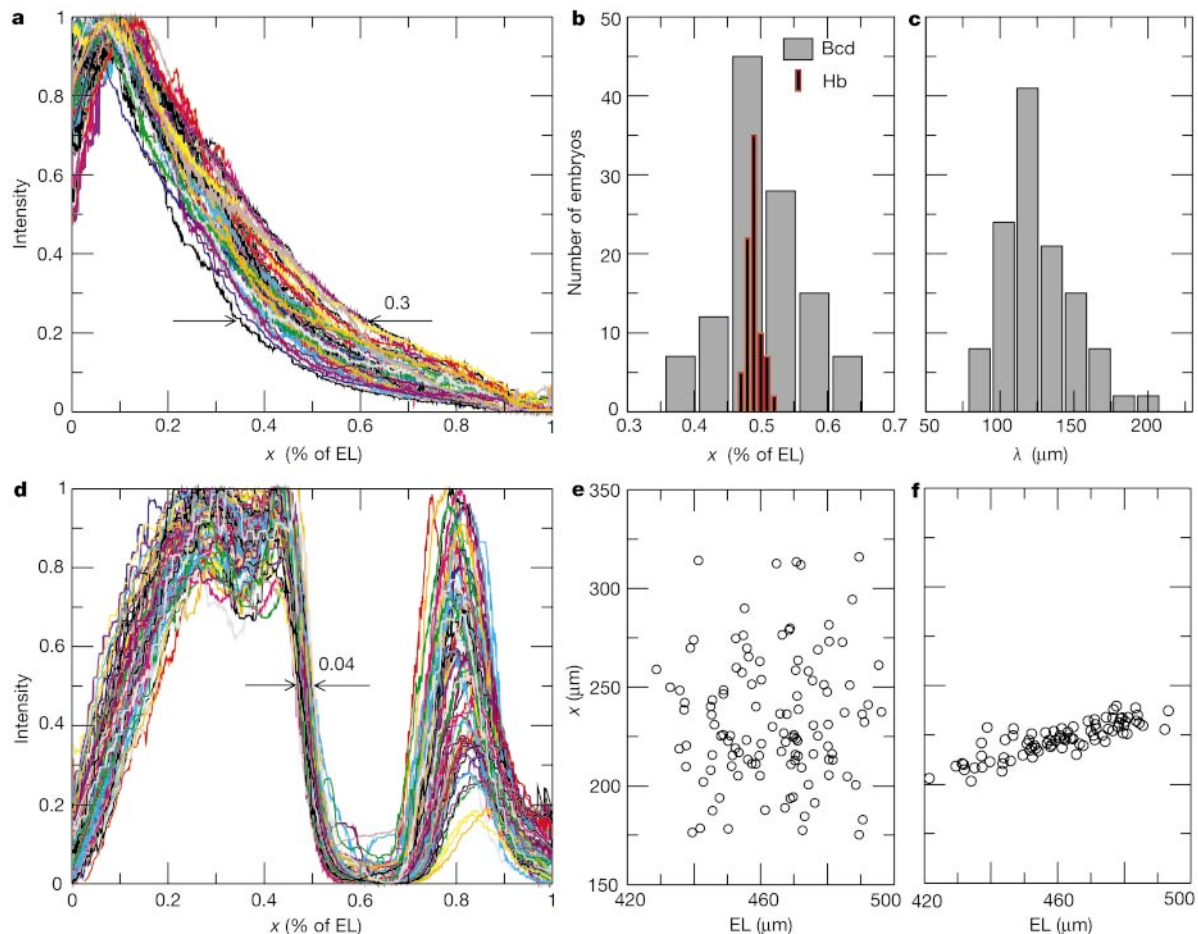

Figure 2 Positional information of Bcd and Hb gradients. **a**, Bcd gradient in about 100 embryos. **b**, Distribution of positions at which each gradient crosses a given threshold: 0.23 for Bcd, 0.5 for Hb. **c**, Distribution of slope of exponential decay for each Bcd profile. **d**, Hb gradient in about 100 embryos. **e**, **f**, Position at which each gradient crosses the given threshold versus embryo length (EL) for Bcd (**e**) and Hb (**f**).
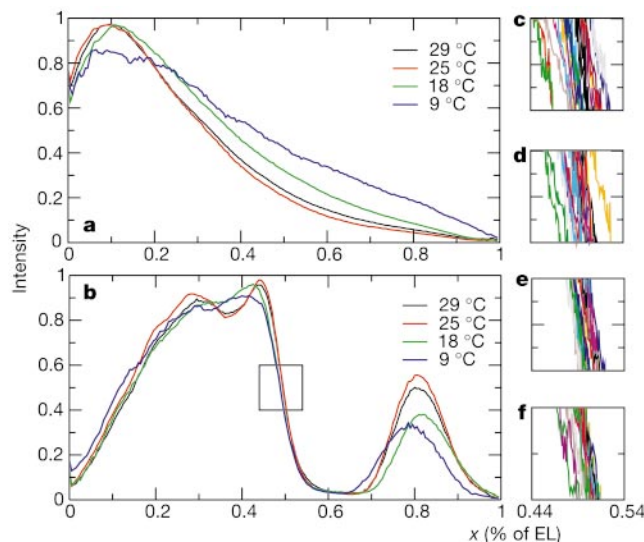
Figure 3 Influence of temperature variation on Bcd and Hb gradients. **a**, Average profiles of Bcd gradients at different temperatures (9–29 °C). **b**, The corresponding average profiles of Hb gradients. **c–f**, Detail of individual Hb profiles at each temperature. Coordinates of the frame correspond to the rectangle shown in **b**. **c**, 9 °C, $\sigma = 0.016$; **d**, 18 °C, $\sigma = 0.013$; **e**, 25 °C, $\sigma = 0.01$; **f**, 29 °C, $\sigma = 0.011$. The average profiles are computed from 18–32 curves.

morphogen model, in which the protease rate, and thus λ, should strongly depend on temperature. However, no change in the position and variability of Hb was observed. Thus, variations due to temperature changes are also compensated at the level of *hb* expression.

To determine when Hb precision arises, we measured gene expression patterns of *bcd* and *hb* in the early embryo from cycle 12 to 14. No significant change was observed in the Bcd pattern during this period: its variability remained extremely high ($\sigma_{Bcd} = 0.07$ EL) and its amplitude remained constant throughout early cycle 14. The first trace of zygotic Hb protein was detected at cycle 13, where the amplitude of the signal increased by a factor of 1.5 above that achieved in unfertilized eggs or in embryos at cycle 11 or 12. At cycle 14, the relative amplitude (compared with cycle 12) of the signal is 3.7 (see Methods for fluorescence quantification). The variability of Hb boundary position (σ_{Hb}) during cycle 13 is 0.015 EL, only slightly higher than that observed during cycle 14, and clearly lower than that of Bcd at any stage in development. The scaling of the Hb boundary position relative to the egg length also appears at cycle 13: no significant correlation existed between the Hb boundary and the size of the egg at cycle 12 ($r_s = 0.3$, $P = 0.1$). At cycle 13, r_s rose to 0.7 ($P = 0.00015$), and further increased to 0.8 during cycle 14.

All the genes downstream of *hb* that we have measured (*Kr*, *kni*, *gt*, *eve*) display the same spatial precision as *hb*. We have used various *Drosophila* mutants to identify additional genes involved in the fine regulation of Hb. Our search assumed that the removal of such genes would increase the variability of Hb to reflect the variability of Bcd itself (note that some genes such as *gt* induce a shift in Hb position, but not in its variability). The best candidate for a maternal posterior gradient is *nanos* (*nos*). The removal of *nos* induces a slight shift in Hb boundary, but the variability at this new position is not significantly changed (Table 2). Moreover, the simultaneous removal of maternal *hb* and *nos* cancels this shift. Hence, the induced shift by *nos* can be attributed to auto-activation of *hb*[7,8]. The removal of *nos* does not abolish the scaling property, and the Hb boundary and EL remain tightly correlated ($r = 0.71$, $r_s = 0.64$, $P < 10^{-5}$). Thus *nos* mutations can modify the average position of the Hb boundary without affecting its precision or scaling.

The natural candidate for zygotic control of Hb is Kruppel (Kr). Double staining for these two gene products shows a strong correlation between the position of their boundaries ($r = 0.90$, $r_s = 0.89$, $P < 10^{-20}$), and regulation of Kr by Hb has been previously demonstrated[9]. Repression of *hb* expression by Kr has also been reported[10]. However, Hb boundary position and its low embryo-to-embryo variability are not affected in *Kr* mutants (Table 2). These results hold even if we consider very late cycle 14 embryos in which other members of gap gene class are active. They seem not to be responsible for the precision of the Hb boundary (Table 2). To test the existence of another, unidentified gene contributing to this process, we removed genes corresponding to about 80% of the *Drosophila* genome by using compound chromosomes, but we observed no effect on the precision of the Hb boundary.

The auto-activation of *hb* by its gene products can be important for the sharpness of the Hb boundary and its average position, but this mechanism alone cannot provide any spatial clue for the precision and scaling. To further investigate this issue, we used embryos homozygous for the *hb*[6N] mutation. These embryos make detectable protein, even though phenotypically the alleles behave as null[11,12]. The boundary of gene expression for these embryos is shifted towards the anterior, reflecting a role for Hb in amplification of its own expression, presumably by the P1 enhancer[8]. The precision and scaling of the Hb boundary in this background,

Table 2 Variability of the Hb boundary

Mutation	x_{Hb}	σ	n
Wild type	0.49	0.010	110
oskar[6]	0.52	0.016	40
nos[BN]	0.54	0.016	16
hb[mat] *nos*[BN]	0.47	0.014	31
exu[PJ42]	0.51	0.020	21
swa[1]	0.52	0.025	17
torso[PM51]	0.50	0.014	30
spg	0.51	0.017	9
Kr[1]	0.49	0.011	29
kni(del)	0.48	0.010	11
gt[YA82]	0.46	0.010	16
hb[6N]	0.45	0.011	17
X⁻	0.43	0.014	40
2R⁻	0.49	0.015	19
2L⁻	0.47	0.014	16
3L⁻	0.50	0.020	39

The average position of the Hb boundary in different zygotic and maternal backgrounds is shown. Anterior = 0; posterior = 1. *n*, number of embryos sampled. Compound chromosomes were used to generate embryos deficient for the X chromosome and individual autosomal arms[18].
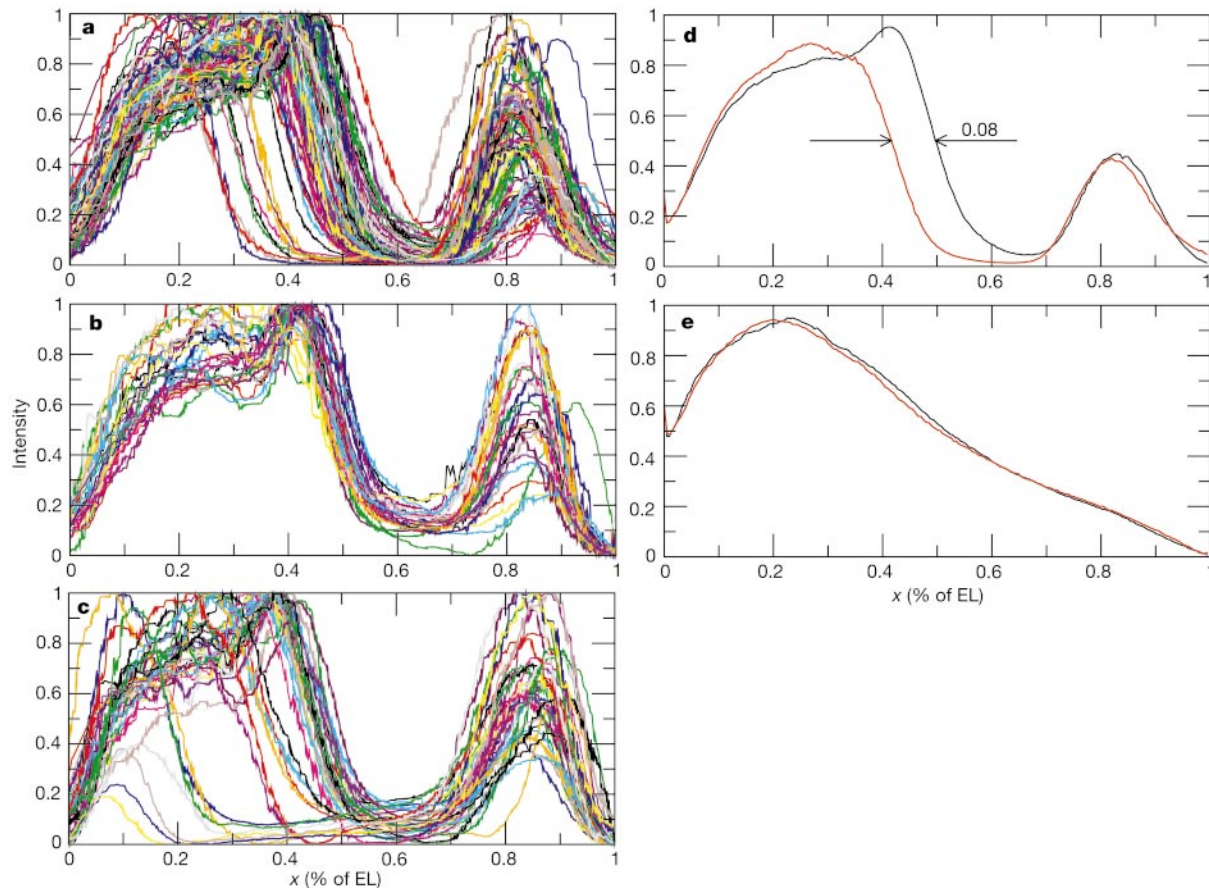
Figure 4 Hb profiles in *staufen* background. **a**–**c**, Hb profiles for about 100 embryos in *stau*^HL (**a**), *stau*^D3 (**b**) and *stau*^r9 (**c**). **d**, Average profile of Hb gradient in *stau*^HL background, for populations shifted forwards and backwards of the average. **e**, The corresponding average Bcd profile for these populations. The average maximum Bcd intensities for these two populations are 1,800 ± 80 (±σ) and 1,750 ± 100.

however, is equal to that of the wild type.

Among all the mutations we have studied, the only ones that affect Hb boundary precision are certain alleles of the maternal gene *staufen* (*stau*). In embryos from mothers homozygous for either *stau*^HL or *stau*^r9, the Hb boundary position shows a variability of 6%, comparable to the observed Bcd variability (Fig. 4a, c). Surprisingly, this variability is largely reduced (to 2%) in another strong allele of *stau*, D3 (Fig. 4b). Mutations in *stau* disrupt *bcd* and *osk* RNAs and decrease Bcd protein level about twofold. We tested whether the effect of *stau* on Hb was simply an indirect effect of its variable effect on bicoid. From the pool of embryos in *stau*^HL background that were double stained for Bcd and Hb, we selected two populations: one that displayed an anterior Hb boundary shift, and one that displayed a posterior shift (Fig. 4d). The corresponding average Bcd profiles for these two populations are very similar, both in the Bcd level and in its spatial distribution (Fig. 4e). Thus, the observed variability in the Hb boundary position may reflect an activity of staufen independent of *bcd*. The disruption of Hb precision in *stau*^HL is transmitted to downstream genes, and is not corrected before gastrulation. For instance, double staining for Hb and Kr (data not shown) shows that the variability of the Kr boundary in the *stau*^HL background is similar to that of the Hb boundary. Moreover, the positions of these two boundaries remain tightly correlated, as in the wild type.

By quantitatively analysing the protein profiles of maternal morphogens and zygotic gap genes in numerous wild-type and mutant embryos, we have demonstrated two phenomena that take place in the early *Drosophila* development. First, at a very early stage, noise associated with the maternal gradient of Bcd is filtered out, and at the same time the genetic network, which includes the Hb gap gene, establishes spatial proportions (scaling) in the embryo. It is potentially significant that *staufen,* the one gene affecting the process, makes a product that localizes to both poles of the egg[13,14]. More work is needed to establish the mechanisms that control the spatial scaling and precision. It would be then interesting to investigate whether similar phenomena are present in other developmental processes in *Drosophila* and other organisms. □

Methods

Immunostaining of embryos

Embryos were collected at 25 °C (except when temperature variations were studied), heat fixed and labelled with fluorescent probes following previously published protocols[15]. All antibodies used were a gift of J. Reinitz and D. Kosman[16].

Image analysis

High-resolution digital images (1,317 × 1,015 pixels, 12 bits per pixel) of stained embryos at the same developmental stage and oriented in a lateral projection were taken. Images were focused at mid-embryo to avoid geometric distortion. Intensity profiles were extracted by sliding a rectangle (the size of a nucleus) perpendicular to the embryo along its edges, and computing the average intensity of its pixels, while projecting the coordinates of its centre on the two (anteroposterior and dorsoventral) axes of the embryo. Two curves, corresponding to dorsal and ventral sides of the embryo, were constituted. For consistency, we compared only dorsal profiles. To normalize the intensity profiles, for each curve the minimum and maximum intensity were computed by the average of the 20 lowest- and highest-intensity pixels (corresponding to the size of one nucleus), and the profiles are linearly mapped to a [0,1] interval. The *x*-axis (when needed) was normalized by the embryo length.

At mid-embryo, the concentration of Hb drops from a high value (normalized to 1) to a low one (normalized to 0). We therefore chose the threshold 0.5 to quantify the spatial position of this boundary. The same threshold is used for the quantification of other gap genes studied.

To characterize Bcd profiles (which are exponential), we chose the threshold for thisprotein ($t = 0.23$) such that, on average, $x_{Bcd} = x_{Hb}$. The measured variability of

letters to nature

Bcd does not depend on the particular choice of t, and other values (such as 0.5) give the same results.

Profile quantification

Fluorescence antibody staining can be used to determine the relative concentration of a protein in a given background compared to the wild type, if a statistical approach is taken: the typical standard deviation for the maximum fluorescence intensity is about 20%. For intensity calibration, we used 20–30 embryos, so the average maximum intensity displays a standard error of 4% ($0.2/\sqrt{25}$). When a background was compared to wild-type embryos, both mutant and wild-type embryos were stained at the same time and in the same conditions. We used Student's t-test to decide whether two averages were different. The position at which the Bcd gradient crosses a given threshold is subject to an error in the normalization process, which we could easily estimate. Supposing that the real concentration in normalized coordinates is $y_{real} = f(x)$, where f varies between 0 and 1, x_0 is computed by solving the equation $f(x_0) = t$, where t is a given threshold. The measured function, using immunofluorescence staining, is $y_{meas} = A_0 f(x) + B_0$, where B_0 is the background due to nonspecific attachment, and A_0 depends on the efficiency of probe–target interaction. The normalization procedure transforms $y_{meas}(x)$ into a normalized function $y_{norm}(x) = (y_{meas}(x) - B)/A$. x_{Bcd} is computed using $y_{norm}(x)$.

The error in the measurement of x_{Bcd} due to error in estimation of A and B is $\Delta x = (1/\mathrm{d}f/\mathrm{d}x|_{x=x_0})(1-t)\Delta B/A_0$, where $\mathrm{d}f/\mathrm{d}x|_{x=x_0}$ is the slope of $f(x)$ at the defining point, and ΔB is the absolute error in estimating B.

The key to reducing the error in the measurement of x_{Bcd} is to have a high signal-to-background ratio ($A/B \cong 8$ in our case). Using the above equation, we find $\Delta x_{Bcd} \cong 1\%$. The real variability of x_{Bcd}, Δ_r, is related to the measured one Δ_m and to error due to normalization Δ_{norm} through $[\mathrm{Delta}]_r^2 = \Delta_m^2 - \Delta_{norm}^2$. Hence, given the precision of our procedure, the error of normalization has a negligible effect on the measured variability of bcd gradient.

A more robust way of measuring the bcd variability is to use the exponential decay of Bcd concentration. Bcd profiles have a peak at about 35 µm (this peak is variable from embryo to embryo) and display a perfect exponential decay after twice this distance. Raw data of immunofluorescence for Bcd are fitted by $I = A \exp(-x/\lambda) + B$ for abscissae beyond twice the peak position. A nonlinear Levenberg–Marquardt fit procedure was used to estimate the parameters. The slope of the exponential, λ, for each embryo was then computed from all values of the raw curve, and did not depend on normalization parameters. The confidence limit of λ in each fitted curve was determined by the curvature matrix of the χ^2 function at its minimum[17], and is smaller than 1 µm (σ_λ for between-embryo variability is 20 µm).

Received 28 August; accepted 4 December 2001.

1. Wolpert, L. Positional information and the spatial pattern of cellular differentiation. *J. Theor. Biol.* **25**, 1–47 (1969).
2. Driever, W. & Nusslein-Volhard, C. The bicoid protein determines position in the *Drosophila* embryo in a concentration-dependent manner. *Cell* **54**, 95–104 (1988).
3. Driever, W. & Nusslein-Volhard, C. A gradient of bicoid protein in *Drosophila* embryos. *Cell* **54**, 83–93 (1988).
4. Struhl, G., Struhl, K. & Macdonald, P. M. The gradient morphogen bicoid is a concentration-dependent transcriptional activator. *Cell* **57**, 1259–1273 (1989).
5. Lacalli, T. C. & Harrison, L. G. From gradient to segments: models for pattern formation in early *Drosophila*. *Semin. Dev. Biol.* **2**, 107–117 (1991).
6. Segel, I. H. *Enzyme Kinetics* (Wiley, New York, 1975).
7. Treisman, J. & Desplan, C. The products of the *Drosophila* gap genes *hunchback* and *Kruppel* bind to the hunchback promoters. *Nature* **341**, 335–337 (1989).
8. Wimmer, E. A., Carleton, A., Harjes, P., Turner, T. & Desplan, C. Bicoid-independent formation of thoracic segments in *Drosophila*. *Science* **287**, 2476–2479 (2000).
9. Struhl, G., Johnston, P. & Lawrence, P. A. Control of *Drosophila* body pattern by the hunchback morphogen gradient. *Cell* **69**, 237–249 (1992).
10. Jackle, H., Tautz, D., Schuh, R., Seifert, E. & Lehmann, R. Cross regulatory interactions among the gap genes of *Drosophila*. *Nature* **324**, 668–670 (1986).
11. Simpson-Brose, M., Treisman, J. & Desplan, C. Synergy between the hunchback and bicoid morphogens is required for anterior patterning in *Drosophila*. *Cell* **78**, 855–865 (1994).
12. Hulskamp, M., Lukowitz, W., Beermann, A., Glaser, G. & Tautz, D. Differential regulation of target genes by different alleles of the segmentation gene *hunchback* in *Drosophila*. *Genetics* **138**, 125–134 (1994).
13. St Johnston, D., Beuchle, D. & Nusslein-Volhard, C. *Staufen*, a gene required to localize maternal RNAs in the *Drosophila* egg. *Cell* **66**, 51–63 (1991).
14. Ferrandon, D., Elphick, L., Nusslein-Volhard, C. & St Johnston, D. Staufen protein associates with the 3'UTR of bicoid mRNA to form particles that move in a microtubule-dependent manner. *Cell* **79**, 1221–1232 (1994).
15. Roberts, D. B. (ed.) *Drosophila, A Practical Approach* (Oxford Univ. Press, Oxford, 1998).
16. Kossman, D., Small, S. & Reinitz, J. Rapid preparation of a panel of polyclonal antibodies to *Drosophila* segmentation proteins. *Dev. Genes Evol.* **208**, 290–294 (1998).
17. Press, W. H., Teukolsky, S. A., Vettering, W. T. & Flannery, B. P. *Numerical Recipes in C* (Cambridge Univ. Press, Cambridge, 1992).
18. Merrill, P., Sweeton, D. & Wieschaus, E. Requirements for autosomal gene activity during precellular stages of *Drosophila melanogaster*. *Development* **104**, 495–509 (1988).

....

Activation-induced cytidine deaminase turns on somatic hypermutation in hybridomas

Alberto Martin*, **Philip D. Bardwell***, **Caroline J. Woo***, **Manxia Fan***, **Marc J. Shulman**† & **Matthew D. Scharff***

* *Department of Cell Biology, Albert Einstein College of Medicine, 1300 Morris Park Avenue Chanin 403, Bronx, New York 10461, USA*
† *Immunology Department, Medical Sciences Building, 1 King's College Circle, University of Toronto, Toronto, Ontario M5S 1A8, Canada*

....

The production of high-affinity protective antibodies requires somatic hypermutation (SHM) of the antibody variable (V)-region genes. SHM is characterized by a high frequency of point mutations that occur only during the centroblast stage of B-cell differentiation. Activation-induced cytidine deaminase (AID), which is expressed specifically in germinal-centre centroblasts[1], is required for this process, but its exact role is unknown[2]. Here we show that AID is required for SHM in the centroblast-like Ramos cells, and that expression of AID is sufficient to induce SHM in hybridoma cells, which represent a later stage of B-cell differentiation that does not normally undergo SHM. In one hybridoma, mutations were exclusively in G·C base pairs that were mostly within RGYW or WRCY motifs, suggesting that AID has primary responsibility for mutations at these nucleotides. The activation of SHM in hybridomas indicates that AID does not require other centroblast-specific cofactors to induce SHM, suggesting either that it functions alone or that the factors it requires are expressed at other stages of B-cell differentiation.

Three human B-cell lines (namely Ramos, BL-2 and CL-01) undergo SHM[3–5], thus opening the possibility of studying this process *in vitro*. We found previously[6] that V-region mutation rates in different Ramos clones were correlated with the level of their AID messenger RNA, suggesting that AID is important in SHM in Ramos cells. Specifically, both the rates of mutation and the mRNA levels of AID for Ramos clones 6 and 7 were higher than those for Ramos clone 1 (Fig. 1a and ref. 6). To determine whether low AID expression was itself responsible for the low mutation rates in Ramos clone 1, this clone was stably transfected with either a vector expressing human AID (hAID) or an empty vector control. Mutation rates of typical transfected clones were then determined by sequencing unselected V regions after 1 or 2 months in culture (Table 1). Clones expressing low levels of AID (that is, clones C.1 and A.1) had very few mutations in the V region, whereas clones that expressed ~25-fold higher levels of AID mRNA (that is, clones A.2 and A.5) had many more V-region mutations (Fig. 1b and Table 1). Table 2 summarizes the mutational features of all the Ramos clones that expressed elevated levels of AID and shows that the rates and characteristics of the mutations in all of these clones were similar: there was a targeting bias of G/C nucleotides, transitions were slightly favoured over transversions, and ~35% of mutations were in G or C nucleotides within RGYW (A/G, G, C/T, A/T) or WRCY hot-spot sequences, motifs that are frequently targeted in SHM both *in vivo* and *in vitro*[7,8]. These results indicate that AID is required for